NDT
Nephrology Dialysis Transplantation

Original Articles

Microvesicles derived from human adult mesenchymal stem cells protect against ischaemia–reperfusion-induced acute and chronic kidney injury

Stefano Gatti[1,*], Stefania Bruno[2,3,*], Maria Chiara Deregibus[2], Andrea Sordi[1], Vincenzo Cantaluppi[2], Ciro Tetta[4] and Giovanni Camussi[2]

[1]Center for Surgical Research, Fondazione IRCCS Cà Granda Ospedale Maggiore Policlinico, Milano, Italy, [2]Department of Internal Medicine and Molecular Biotechnology Center, University of Torino, Italy, [3]Sis-Ter S.p.A., Palazzo Pignano, Crema, Italy and [4]Fresenius Medical Care, Bad Homburg, Germany, UK

Correspondence and offprint requests to: Giovanni Camussi; E-mail: giovanni.camussi@unito.it
[*]Both authors contributed equally to this work.

Abstract

Background. Several studies demonstrated that mesenchymal stem cells (MSCs) reverse acute kidney injury (AKI) by a paracrine mechanism rather than by MSC transdifferentiation. We recently demonstrated that microvesicles (MVs) released from MSCs may account for this paracrine mechanism by a horizontal transfer of messenger RNA and microRNA.

Methods. MVs isolated from MSCs were injected intravenously in rats (30 μg/rat) immediately after monolateral nephrectomy and renal artery and vein occlusion for 45 min. To evaluate the MV effects on AKI induced by ischaemia–reperfusion injury (IRI), the animals were divided into different groups: normal rats ($n = 4$), sham-operated rats ($n = 6$), IRI rats ($n = 6$), IRI + MV rats ($n = 6$), and IRI + RNase-MV rats ($n = 6$), and all animals were sacrificed at Day 2 after the operation. To evaluate the chronic kidney damage consequent to IRI, the rats were divided into different groups: sham-operated rats ($n = 6$) and IRI rats ($n = 6$), IRI + MV rats ($n = 6$), and all animal were sacrificed 6 months after the operation.

Results. We found that a single administration of MVs, immediately after IRI, protects rats from AKI by inhibiting apoptosis and stimulating tubular epithelial cell proliferation. The MVs also significantly reduced the impairment of renal function. Pretreatment of MVs with RNase to inactivate their RNA cargo abrogated these protective effects. Moreover, MVs by reducing the acute injury also protected from later chronic kidney disease.

Conclusion. MVs released from MSCs protect from AKI induced by ischaemia reperfusion injury and from subsequent chronic renal damage. This suggest that MVs could be exploited as a potential new therapeutic approach.

Keywords: acute kidney injury; chronic kidney disease; ischaemia–reperfusion injury; mesenchymal stem cells; microvesicles

Introduction

Bone marrow (BM) mesenchymal stem cells (MSCs) were extensively investigated for their reparative, regenerative and immunomodulatory properties [1,2]. Several studies, using different animal models of diseases, showed that treatment with exogenous MSCs ameliorates acute kidney injury (AKI) [3–8]. Moreover, few studies addressed the potential beneficial effects of MSC treatment in chronic kidney disease (CKD) [9–14]. The effect of MSCs both in the acute and chronic models was related to a paracrine action rather than a transdifferentiation into renal resident cells [15–21]. In this context, MSCs may act by mitigating injury and/or favouring repair by delivering critical signals to the differentiated cells which survived the injury. These may include soluble factors that in a paracrine or even endocrine manner modify the cell behavior favouring kidney recovery [5,15–21]. Recent studies have suggested that cells may communicate also by circular membrane fragments called microvesicles (MVs) [22]. We recently demonstrated that MVs released from MSCs may mimic the beneficial effect of MSC treatment in a glycerol-induced model of AKI [23]. In this model, MVs induced epigenetic changes in resident cells by delivering their messenger RNA (mRNA) cargo leading to reentry into the cell cycle and activation of tissue regenerative programmes [23].

MVs may originate either as exosomes derived from the endosomal compartment [24,25] or as shedding vesicles from direct budding of the cell plasma membrane [26,27].

MVs released from a given cell type may interact through specific receptor ligands with other cells transfer-

ring proteins, biological reactive lipids and receptors [27,28]. It has been recently shown that MVs may also transfer mRNAs and microRNAs (miRNA) that may account for epigenetic changes in target cells [29–31]. Ratajczak *et al.* [29] first demonstrated that MVs derived from murine embryonic stem cells may induce reprogramming of haemopoietic progenitor cells. We found that MVs derived from endothelial progenitor cells may activated an angiogenic programme in endothelial cells by a horizontal transfer of mRNA [30]. More recently, we demonstrated that MVs derived from human stem cells may also deliver human mRNA to mouse cells *in vivo*, resulting in protein translation [31,32]. Yuan *et al.* [33] showed that besides mRNA, MVs may transfer in target cells also miRNA that may modulate their phenotype. Recent studies by Quesemberry and Aliotta [34–37] proposed that MVs play a critical role in the continuum model of stem cell biology.

The aim of the present study was to evaluate whether the administration of MVs derived from MSCs may favour the recovery of AKI and CKD induced by ischaemia–reperfusion injury (IRI).

Methods

Isolation and characterization of BM-MSCs

MSCs were obtained from Lonza (Basel, Switzerland), cultured and characterized as previously described [23]. MSCs were used until the 6th passage of culture. All the cell preparations at different passages of culture expressed the typical MSC markers: CD105, CD73, CD44, CD90, CD166 and CD146. They also expressed Human Leucocyte Antigen (HLA) Class I. BM-MSC preparations did not express a haematopoietic markers like CD45, CD14 and CD34. They also did not express the co-stimulatory molecules (CD80, CD86 and CD40), HLA Class II and the endothelial markers (CD31, von Willebrand Factor and Vascular Endothelial Growth Factor Receptor 2). The adipogenic, osteogenic and chondrogenic differentiation ability of MSCs was determined as previously described [23].

Human fibroblasts, used as control, were isolated from dermas and cultured as described [38].

Isolation and characterization of MVs

MVs obtained from supernatants of MSCs or fibroblasts (F) (cell viability >99% as detected by trypan blue exclusion), were isolated by differential ultracentrifugation and characterized as previously described [23]. Briefly, MVs were obtained from supernatants of MSCs or of fibroblasts (F), cultured overnight in RPMI deprived of fetal calf serum and supplemented with 0.5% of bovine serum albumin (Sigma). After centrifugation at 2000 *g* for 20 min to remove debris, cell-free supernatants were centrifuged at 100 000 *g* (Beckman Coulter Optima L-90K ultracentrifuge) for 1 h at 4°C, washed in serum-free medium 199 containing HEPES 25 mM (Sigma) and submitted to a second ultracentrifugation in the same conditions. The protein content of MVs was quantified by Bradford method (BioRad, Hercules, CA). Endotoxin contamination of MVs was excluded by Limulus test (Charles River Laboratories, Inc., Wilmington, MA). By Zetasizer Nano (Malvern Instruments, Malvern Worcestershire, UK), transmission and scanning electron microscopy, the size of MVs ranged from 80 nm to 1 μm, with a mean value of 135 nm [23]. Cytofluorimetric analyses showed the presence of several adhesion molecules such as CD44, CD29, α4- and α5-integrins and CD73, but not α6-integrin [23]. In addition, MVs did not express HLA Class I at variance with the cells of origin or HLA Class II. We previously characterized the MV content of mRNA by microarray analysis [23] and of miRNA as well [39].

In selected experiments, MVs were treated with 1 U/mL RNase (Ambion Inc., Austin, TX) for 3 h at 37°C and the reaction was stopped by addition of 10 U/mL RNase inhibitor (Ambion Inc.) and MVs were washed by ultracentrifugation [23]. The efficacy of RNase treatment was evaluated by MV–RNA analyses by Agilent 2100 bioanalyser (Agilent Tech. Inc., Santa Clara, CA). Moreover, after RNA extraction using TRIZOL reagent (Invitrogen), spectrophotometer analysis was performed of total extracted RNA (untreated: 1.4 ± 0.19 μg RNA/mg protein MV;

RNase treated: <0.2 μg RNA/mg protein MV). In addition, RNA extracted from RNase-treated and -untreated MVs was labeled by oligo-dT-driven retrotranscription and analysed on 0.6% agarose gel to show the complete degradation of RNA by RNase treatment as previously described [23].

To trace *in vivo* MVs by fluorescent microscopy, MVs were labeled with PKH26 dye (Sigma) as previously described [23].

Animal model of monolateral kidney IRI

All animals received care in compliance with the Principles of Laboratory Animal Care (NIH publication no. 86–23, revised 1985) and the institutional review board approved the protocol.

Male Sprague–Dawley rats (250 g body weight) were anaesthetized with isoflurane and N_2O/O_2, maintained at 37°C under continuous monitorization, and the fluid loss during surgery was replaced with 1–2 mL saline. The right kidney was removed by a subcapsular technique and the left renal artery and vein were occluded for 45 min by using a nontraumatic vascular clamp. Rats were housed individually in a ventilated cage system [Tecniplast, Buguggiate (Va), Italy] at $22 \pm 1°C$, $55 \pm 5\%$ humidity, on a 12-h dark/light cycle, and were allowed free access to rat chow and water *ab libitum*.

To evaluate the AKI induced by IRI, the animals were divided into different groups: normal rats ($n = 4$); sham-operated rats: right nephrectomy without clamp and sacrificed at Day 2 after operation ($n = 6$); IRI rats: right nephrectomy and clamp of left renal pedicle for 45 min and sacrificed at Day 2 after operation ($n = 6$) rats; IRI + MV rats: right nephrectomy and clamp of left renal pedicle for 45 min, injected intravenously immediately with 30 μg of MVs and sacrificed at Day 2 after operation ($n = 6$); IRI + RNase-MV rats: right nephrectomy and clamp of left renal pedicle for 45 min, injected intravenously immediately after IRI with 30 μg of MVs, pretreated with RNase and sacrificed at Day 2 after operation ($n = 6$) and IRI + F-MV rats: right nephrectomy and clamp of left renal pedicle for 45 min, injected intravenously immediately with 30 μg of MVs from fibroblasts (F-MV) and sacrificed at Day 2 after operation ($n = 6$). Six rats per group were studied at Day 7 after induction of AKI to evaluate renal function and morphology.

To evaluate the CKD induced by IRI, the rats were divided into different groups: sham-operated rats: right nephrectomy without clamp and sacrificed 6 months after the operation ($n = 6$); IRI rats: right nephrectomy and clamp of left renal pedicle for 45 min and sacrificed 6 months after the operation ($n = 6$) and IRI + MV rats: right nephrectomy and clamp of left renal pedicle for 45 min rats, injected intravenously immediately after IRI with a single dose of 30 μg of MVs and sacrificed 6 months after the operation ($n = 6$).

MVs were injected at a dose of 30 μg of MV protein/rat, that were produced overnight by ~150 000 MSCs in serum starved condition.

Renal function

Blood samples for measurement of blood urea nitrogen (BUN) and plasma creatinine were collected at 2 days and 6 months after IRI. Serum creatinine was measured using a colorimetric microplate assay based on the Jaffe reaction (Quantichrom Creatinine Assay; BioAssay Systems, Hayward, CA). BUN was measured by direct quantification of serum urea with a colorimetric assay kit according to the instruction protocol (Quantichrom Urea Assay; BioAssay Systems). Urine was collected (24 h) to determine urinary protein by Bradford method and creatinine excretion.

Renal morphology

For renal histology, 5-μm-thick paraffin kidney sections were routinely stained with hematoxylin and eosin (Merck, Darmstadt, Germany). Luminal hyaline casts and cell lose (denudation of tubular basement membrane) were assessed in nonoverlapping fields (up to 28 for each section) using a ×40 objective [high-power filed (HPF)] to evaluate the score of the AKI. Number of casts and tubular profiles showing necrosis were recorded in a single-blind fashion [8]. To evaluate the score of CKD, semiquantitative evaluation, based on arbitrary scores, was performed by a blinded observer. The scores for interstitial lymphocytic infiltrates, interstitial fibrosis and tubular atrophy ranged from 0 to 3+ as follows—0: no changes, 1+: damage to <25% of the interstitial area; 2+: damage to 25–50% of the interstitial area and 3+: damage to >50% of the interstitial area. The scores were assessed in nonoverlapping fields (up to 10 for each section) using a ×40 objective (HPF). [13]. Glomerular sclerosis was defined as the presence of dense abundant deposition of Periodic acid-Schiff (PAS) positive material at the glomerular tuft, with occlusion of capillary loops and segmental hyalinization in 100 consecutive glomeruli by determining the percentage of

glomeruli exhibiting sclerotic lesion [12]. Immunohistochemistry for detection of proliferation of tubular cells was performed as Bromodeoxyuridine (BrdU) incorporation or staining for proliferating cell nuclear antigen (PCNA) (monoclonal anti-PCNA antibody; Santa Cruz Biotechnology, Santa Cruz, CA) as previously described [16,23]. Apoptosis was measured by terminal transferase-mediated deoxyuridine triphosphate nick-end-labeling (TUNEL) assay (ApopTaq Apoptosis Detection Kit; Millipore Inc., Billerica, MA) according to the manufacturers' protocol. Scoring for BrdU-positive, PCNA-positive and TUNEL-positive cells was carried out by counting the number of positive nuclei per field in 10 randomly chosen sections of kidney cortex using ×40 magnification.

Confocal microscopy analysis (Zeiss LSM 5 Pascal; Carl Zeiss International, Oberkochen, Germany) was performed on frozen sections for localization of PKH26-labeled MVs in different organs as previously described [23]. Nuclei were stained with Hoechst 33258 dye (Sigma).

Statistical analysis

Statistical analysis was performed by using the *t*-tests, analysis of variance (ANOVA) with Newmann–Keuls' or ANOVA with Dunnet's multicomparison tests as appropriate. A P-value of <0.05 was considered significant.

Results

MVs derived from MSCs protect against AKI induced by ischaemia–reperfusion

A significant rise in BUN and creatinine was observed 2 days after induction of IRI (Figure 1). This was associated with a marked tubular epithelial injury characterized by tubular apoptosis and necrosis, loss of brush border, detachment of tubular epithelial cells and presence of proteinaceous casts into tubules (Figure 1). Sham-operated rats displayed no significant functional or histological alterations (Figure 1). In IRI rats injected with 30 μg of MVs immediately after reflow, the tubular lesions observed after 2 days were significantly reduced in respect to IRI rats treated with vehicle alone (Table 1 and Figure 1). In addition, IRI rats treated with MVs had significantly lower serum creatinine and BUN at Day 2 after MV injection than IRI rats injected with vehicle alone (Figure 1).

IRI rats treated with MVs had significantly higher PCNA staining and BrdU incorporation within tubules in respect to IRI rats untreated with MVs, suggesting that MVs enhanced tubular cell proliferation (Figure 2). Moreover, apoptotic cells were reduced in IRI rats treated with MVs, suggesting an anti-apoptotic effect of MVs on tubular cells (Figure 3).

When MVs were incubated with RNase, the *in vivo* effect on functional and morphological recovery was reduced. As shown in Table 1 and Figure 1, RNase treatment significantly reduced the recovery of BUN and creatinine as well as of tubular lesions. In fact, at Day 2, the renal histology showed marked tubular epithelial injury, as observed in untreated IRI rats (Table 1 and Figure 1). Tubular cell proliferation (Figure 2), and apoptosis (Figure 3), did not significantly differ in rats injected with RNase-treated MVs from that of untreated rats with IRI.

The specificity of MSC-derived MVs was indicated by the absence of protective effects of MVs derived from human fibroblasts (F-MV) (Table 1 and Figures 1–3).

Using MVs labeled with PKH26, we evaluated by confocal microscopy their localization in different organs of IRI rats, at different time points (2, 6 and 24 h). MVs were detected in the ischaemic kidney already 2 h after the injec-

tion and persisted for 6 h but were not more detectable 24 h after injection (Figure 4A–C). At 2 and 6 h after the injection, some MVs were detected within glomeruli, but the majority of them were within tubules (Figure 4A and B). When labeled, MVs were injected into normal control rats, and the renal accumulation was minimal (Figure 4D). In contrast, liver accumulation of MVs was detected both in normal and in IRI rats (Figure 4E and F). The accumulation in the spleen was similar to that observed in the liver, whereas MVs were minimally detected in the lung capillaries (data not shown). Twenty-four hours after injection, MVs were no longer detectable either in normal or AKI rats in any organs.

The functional and morphological recovery was complete at Day 7 in both groups of IRI rats, treated or not with MVs (creatinine: 0.6 ± 0.39 and BUN: 45 ± 5.5).

MSC-derived MVs protect against CKD induced by IRI

We evaluated the development of CKD in our model of IRI. IRI rats showed significantly higher levels of serum creatinine and BUN than sham-operated rats and normal controls after 6 months from the operation (Figure 5A and B). At this time point, IRI rats showed only some mesangial accumulation of matrix in glomeruli (Figure 6E) but focal lymphocyte interstitial infiltrates and abundant matrix deposition associated with areas of tubular atrophy and presence of cystic formations (Figure 6A and B).

To test the possibility that MV treatment might protect against CKD development after IRI-induced AKI, we evaluated the renal function and histology 6 months after IRI in rats treated or not with MVs and in sham-operated rats. After this period of time, the mean body weight did not differ among the different experimental groups (sham: 585 ± 15 g; IRI: 595 ± 32 g and IRI + MV: 586 ± 24 g).

Rats treated with a single intravenous injection of 30 μg of MVs immediately after IRI showed significantly lower levels of BUN and creatinine than IRI rats untreated with MVs (Figure 5A and B).

No significant difference in 24-h urine volume was observed among the different experimental groups (sham: 17.3 ± 1.8 mL; IRI: 17.6 ± 1.28 mL and IRI + MV: 17.1 ± 0.89 mL). Urine analyses showed that untreated IRI rats developed proteinuria when compared with sham-operated rats. Proteinuria in MV-treated IRI rats was significantly lower than that in untreated IRI rats as it was similar to that of sham-operated rats (Figure 5C). Urinary total proteins/creatinine ratios in the MV-treated rats were significantly lower than that in IRI-untreated rats (Figure 5D).

The kidneys of MV-treated rats subjected to IRI showed less fibrosis when compared with untreated IRI rats. Moreover, interstitial lymphocyte infiltrates, tubular atrophy and cystic formation were almost absent (Figure 6D and Table 2). In addition, MV-treated rats showed substantial reduction in the accumulation of matrix in the glomeruli in respect to IRI-untreated rats (Figure 6E and F and Table 2).

Discussion

In the present study, we demonstrated that a single administration of MVs derived from MSCs, immediately after induction of IRI, protects rats against AKI and CKD.
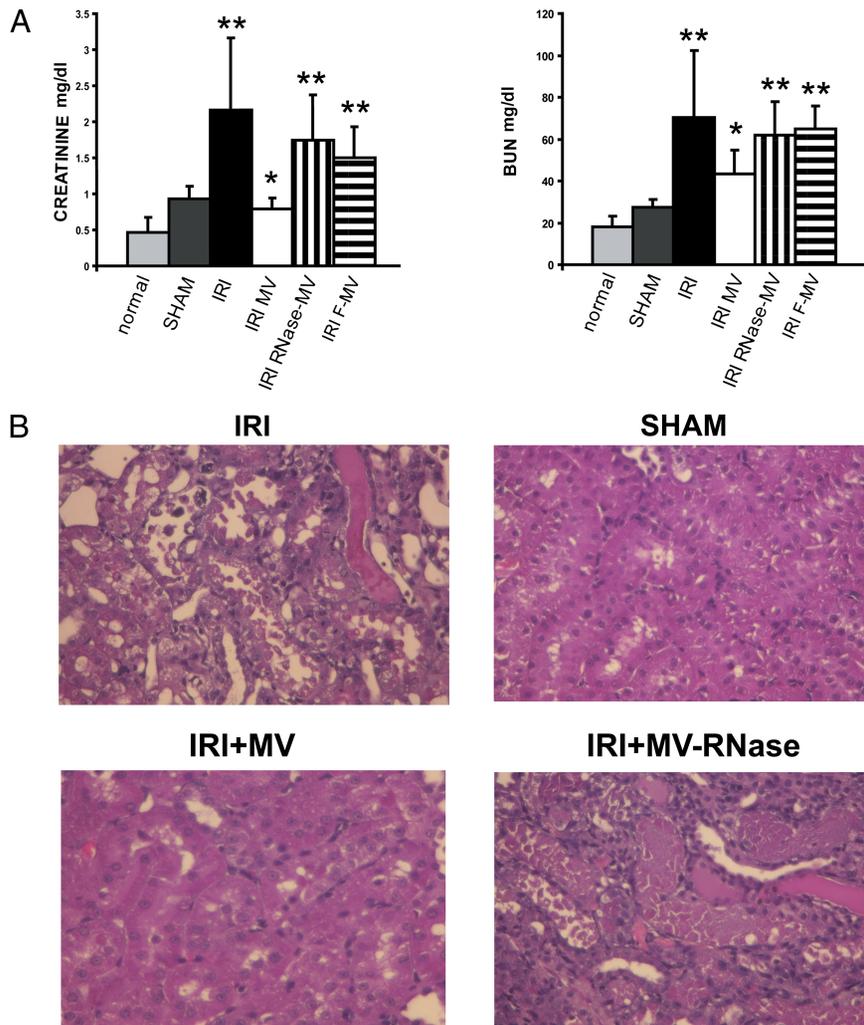
Fig. 1. Effects of intravenous injection of MVs from human MSCs in rats with AKI induced by ischaemia–reperfusion. (**A**) Creatinine and BUN values at Day 2 after IRI. ANOVA with Dunnet's multicomparison test: *P < 0.05 MV-treated IRI rats versus IRI rats; **P < 0.05 IRI rats treated or not with RNase-MV and IRI rats treated with F-MV versus normal and sham-operatedrats. (**B**) Representative micrographs of renal histology at Day 2 after IRI in IRI rats, in sham-operated rats and in IRI rats injected with 30 μg of MVs or RNase-MV. Original magnication: ×400.Normal = healthy rats = right nephrectomy without clamp; IRI = IRI injected with saline alone; IRI + MV = IRI rats treated with 30 μg MVs; IRI + RNase-MV = IRI rats treated with 30 μg RNase-inactivated MVs.

Table 1.. Effect of MVs on renal morphology at Day 2 after IRI[a,b]

2 days	Normal	IRI	Sham	IRI + MV	IRI + RNase-MV	IRI + F-MV
Cast (n/HPF)	0	2.3 ± 1.5	0	*0.45 ± 0.2	2.75 ± 0.9	2.1 ± 1.2
Tubular necrosis (n/HPF)	0	2.7 ± 0.35	0	*0.41 ± 0.19	2.6 ± 0.82	2.4 ± 0.85

[a]Results are expressed as mean ± SD; ANOVA with Dunnet's multicomparison test: *P < 0.05 treatments versus untreated IRI.
[b]IRI + MV = IRI-treated MSC-derived MVs; IRI + RNase-MV = IRI treated with RNase-treated MSC-derived MVs; IRI + F-MV = IRI treated with fibroblast-derived MVs; HPF= high power field.

Several studies demonstrated that the administration of MSCs reverses AKI in different experimental models and protects against CKD [3–14]. These beneficial effects were shown to be associated with a transient recruitment of MSCs within the kidney with a minimal incorporation in the regenerating tubules [5,40,41]. Based on this observation and on findings indicating that tubular repopulation after AKI depends on the reentry into cycle of renal tubular cells survived to injury [42,43], it has been suggested that MSCs may provide a paracrine support to kidney repair [41]. Consistently, Bi *et al.* [20] demonstrated that the administration of conditioned medium from MSCs may mimic the beneficial effects of the stem cell therapy indicating that the tubular engraftment of the MSCs is not necessary. We recently reported that intravenous administration of MVs derived from human MSCs has the
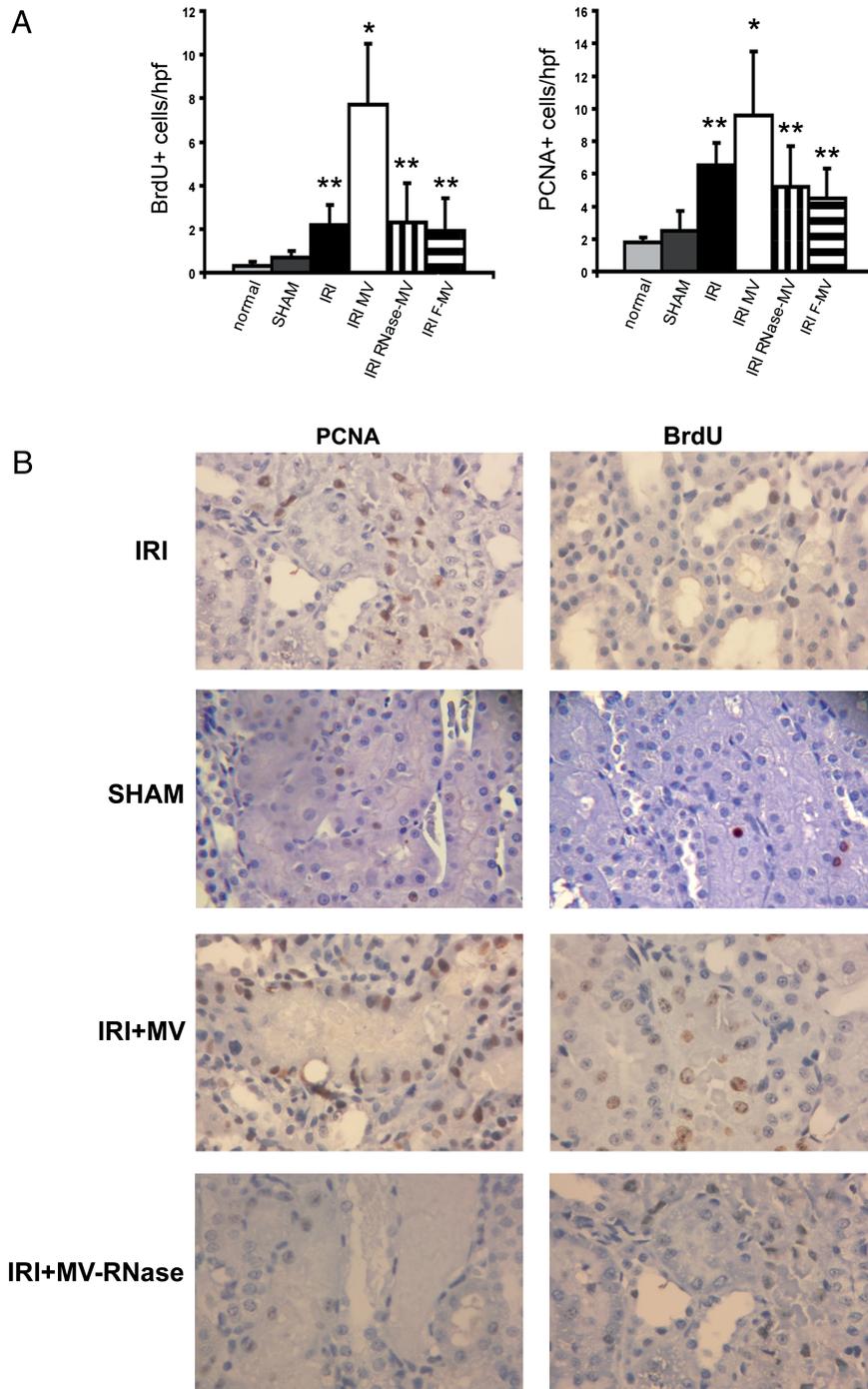
Fig. 2. Renal cell proliferation in IRI rats untreated or treated with MVs. (**A**) Quantification of BrdU- and PCNA-positive cells/HPF. BrdU was injected intraperitoneally for 2 successive days before rats being killed. All quantitative data were obtained from six different rats for experimental conditions. ANOVA with Dunnet's multicomparison test: *$P < 0.05$ MV-injected mice versus IRI control rats; **$P < 0.05$ IRI rats treated or not with RNase-MV and IRI rats treated with F-MV versus normal and sham-operated rats. (**B**) Representative micrographs of PCNA or BrdU uptake staining performed on sections of kidneys 2 days after IRI treated or not with 30 μg of MVs. Normal = healthy rats; sham = right nephrectomy without clamp; IRI = IRI injected with saline alone; IRI + MV = IRI rats treated with 30 μg MVs; IRI + RNase-MV = IRI rats treated with 30 μg RNase-inactivated MVs.

same efficacy of MSCs on the functional and morphological recovery of glycerol-induced AKI in severe combined immunodeficient mice [23].

MVs are small vesicles released by cells bearing the surface antigens characteristic of the cell of origin [27,28,44]

that may enter the target cells through specific receptor–ligand interactions transferring receptors, proteins and bioactive lipids [28]. Moreover, it has been shown that MVs may deliver selected patterns of mRNA and miRNA acting as a new mechanism of genetic exchange between cells

A

B
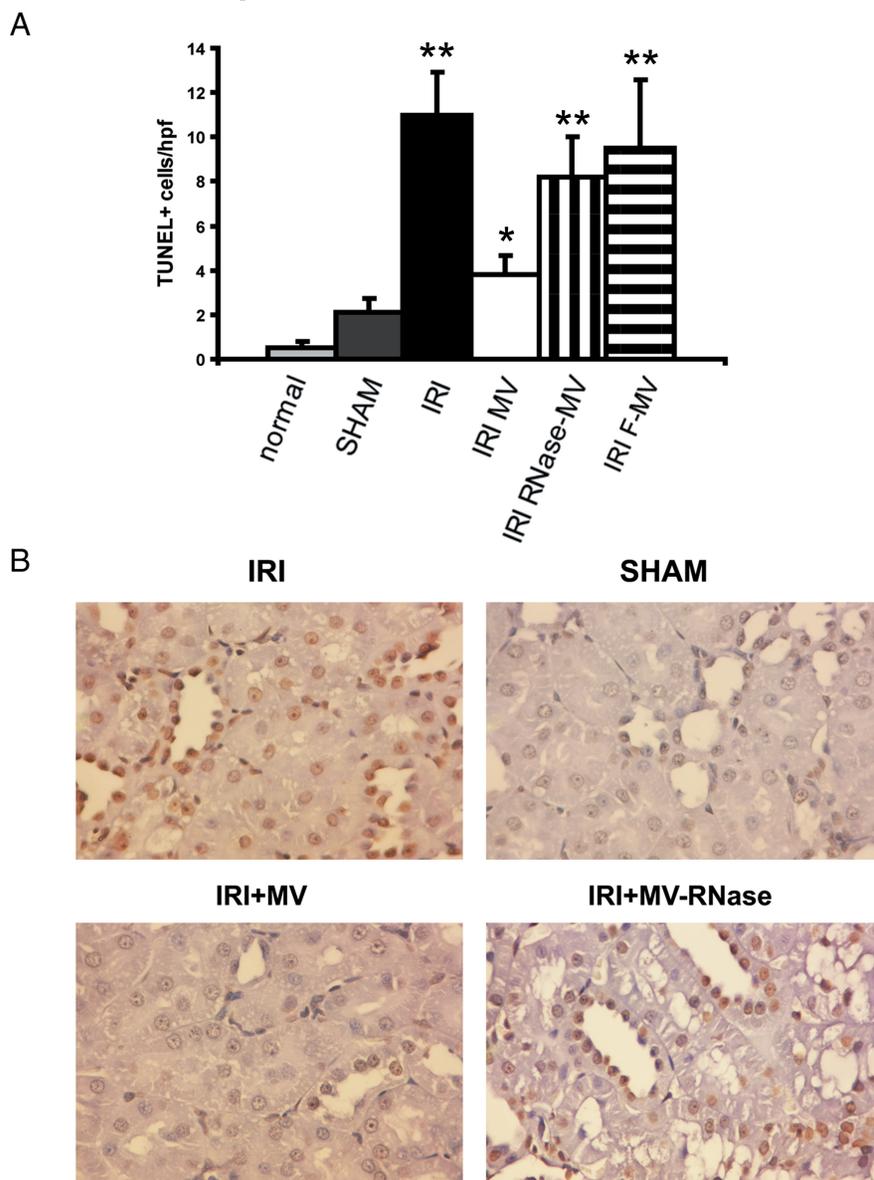
Fig. 3. Renal cell apoptosis in IRI rats untreated or treated with MVs. (**A**) Quantification of TUNEL-positive cells/HPF. All quantitative data were obtained from six different rats for experimental conditions. ANOVA with Dunnet's multicomparison test: *P < 0.05 MV-injected mice versus IRI control rats; **P < 0.05 IRI rats treated or not with RNase-MV and IRI rats treated with F-MV versus normal and sham-operated rats. (**B**) Representative micrographs of TUNEL assay performed on sections of kidneys 2 days after IRI treated or not with 30 μg of MV. Normal = healthy rats; sham = right nephrectomy without clamp; IRI = IRI injected with saline alone; IRI + MV = IRI rats treated with 30 μg MVs; IRI + RNase-MV = IRI rats treated with 30 μg RNase-inactivated MVs.

[29,30]. We recently demonstrated the MV-mediated transfer of functional mRNAs both *in vitro* and *in vivo* [23,32] and of miRNAs *in vitro* [39].

The present study extends the effect of MSC-derived MVs to a model of kidney injury induced by ischaemia–reperfusion. In this model, MVs were found to prevent AKI. After injection, MVs accumulated transiently within glomeruli and injured tubules and stimulated tubular cell proliferation. In addition, MVs may act by a mechanism of renal protection that limits the extent of injury as they significantly reduced tubular cell apoptosis. These biological effects were specific for MSC-derived MVs as MVs obtained from fibroblasts

were ineffective. It is known that MVs protect RNA from physiological concentrations of RNAse. However, as seen in previous studies [23,30,32], pretreatment of MVs with high concentrations of RNase inactivate RNAs. This reduces the biological effect of MVs based on the delivery of RNAs to target cells [23,30,32]. We previously demonstrated that size and expression of surface adhesion molecules did not change in RNase-treated MVs. Moreover, internalization of RNase-treated MVs in target cells did not differ from that of untreated MVs [23]. Here, we show that RNASe-treated MVs lost their protective effect on functional and morphological alterations induced by IRI. Indeed, MVs derived from MSCs con-
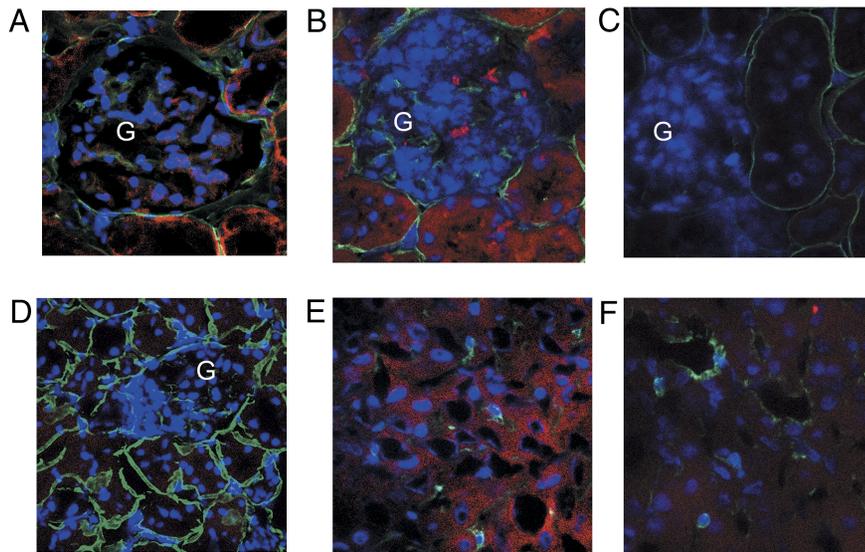
Fig. 4. Detection of MVs after *in vivo* injection. (**A–F**) Representative confocal micrographs of frozen tissue sections of mice injected with PKH26-labeled MVs (red) and stained with laminin antibodies (green staining). MVs were detectable, after 2 h within glomeruli and within the lumen of tubules (**A**); after 6 h, several tubular cells contained red MVs (**B**); at 24 h (**C**), red MVs were not detectable in kidneys of IRI rats. In a normal control rat, red MVs were not detected in tubular cells (**D**). Liver accumulation of red MVs was detected in IRI rats 6 and 24 h after injection (**E** and **F**). Nuclei were counterstained with Hoechst dye; original magnifications: ×400. Per each time points, two animals were studied with similar results.
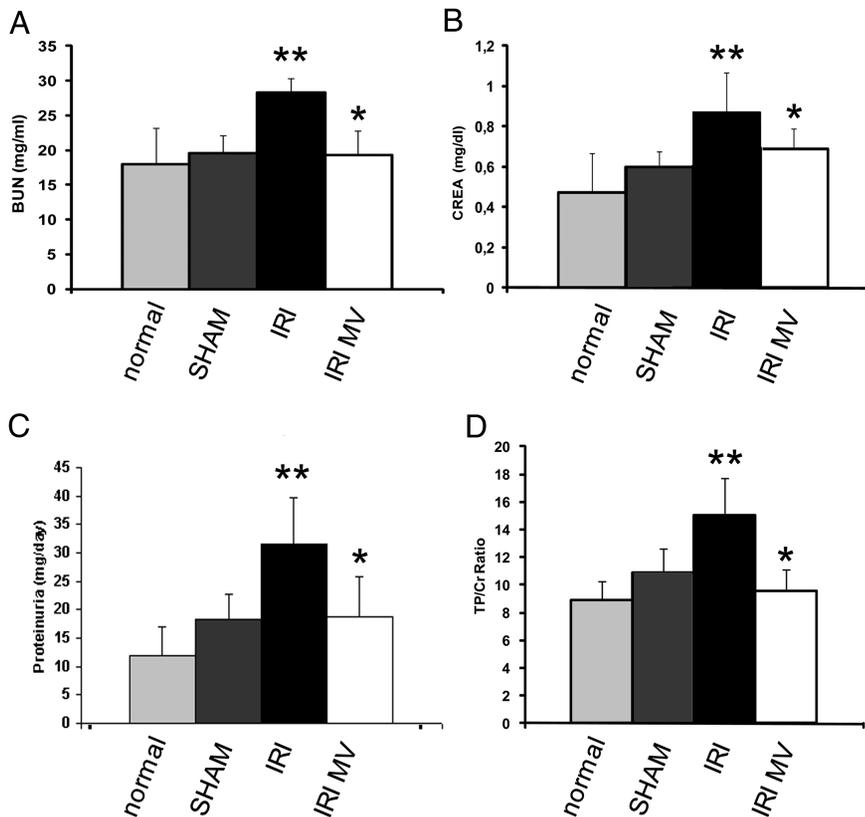
Fig. 5. Renal function parameters 6 months after IRI and MV treatment. (**A**) BUN; (**B**) creatinine; (**C**) proteinuria in 24-h urine collection; (**D**) proteinuria/creatinine (mg/mg) ratio in 24-h urine collection. All quantitative data were obtained from six different rats for each experimental conditions. ANOVA with Dunnet's multicomparison test: *$P < 0.05$ MV-injected mice versus IRI control rats; **$P < 0.05$ IRI rats versus normal and sham-operated rats. Normal = healthy rats; sham = right nephrectomy without clamp; IRI = IRI injected with saline alone; IRI + MV = IRI rats treated with 30 µg MVs.
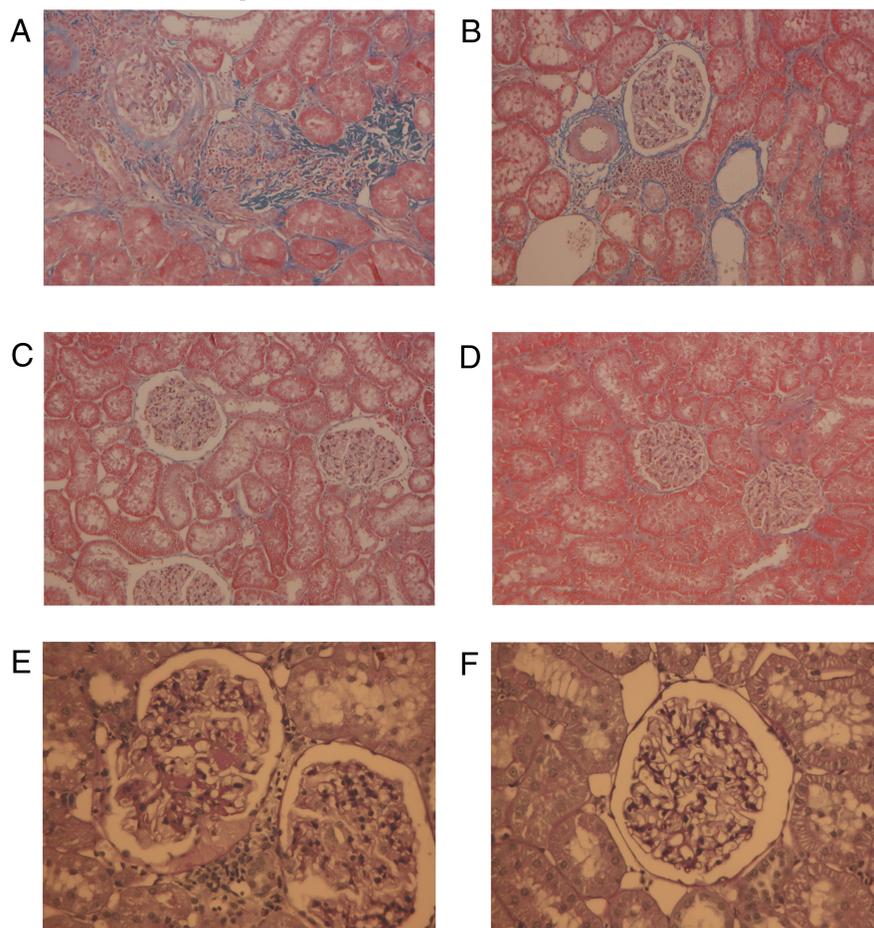
Fig. 6. Renal morphology 6 months after IRI and MV treatment. (**A–D**) Representative photographs of Masson's trichrome-stained kidney sections at 6 months post-IRI to visualize interstitial lymphocyte infiltrates, tubular atrophy and cystic formation: control IRI rat injected with saline alone (**A** and **B**); sham-operated rat (**C**) and IRI rat injected with MVs (**D**). (**E** and **F**) Representative photographs of PAS-stained kidney sections at 6 months post-IRI to asses the degree of glomerular sclerosis: IRI rat injected with saline alone (**E**); IRI rat injected with MVs (**F**); magnification: ×400.

Table 2. Histological assessment of renal damage 6 months after IRI in the MV-treated group versus the untreated group[a,b]

6 months	ILI	IF	TA	% GS
Sham	0	0	0	0
IRI	2.4 ± 0.5	1.5 ± 0.5	2.1 ± 0.4	19 ± 4.5
IRI + MVs	0.2 ± 0.1*	0.7 ± 0.3*	0.2 ± 0.1*	7 ± 2.5*

[a]Results are expressed as mean ± SD; ANOVA with Dunnet's multicomparison test: *$P < 0.05$ treatments versus untreated IRI.
[b]ILI, interstitial lymphocyte infiltration; IF, interstitial fibrosis; TA, tubular atrophy; % GS, percentage of glomerular sclerosis.

tained mRNA involved in the control of transcription, proliferation and cell immune regulation [23] and miRNAs involved in multi-organ development, cell survival and differentiation [39]. Few selected miRNAs were also associated with the regulation of the immune system [39]. Taken together, these observations open new research perspectives on the use of MVs to transfer RNA-based information from stem cells/precursors to target differentiated cells.

It has been previously shown that after an initial recovery in IRI-induced AKI, renal fibrosis and chronic injury may develop [45,46]. In the present study, we found that a single injection at the time of IRI of MVs purified from MSCs not only prevents AKI but also CKD, indicating that

limiting the initial injury may also protect the kidney from development of chronic injury.

In conclusion, MVs released from MSCs mimic the effect of the cells suggesting that they could be exploited as a new therapeutic approach for regenerative medicine. An advantage of using MVs rather than the MSCs themselves is to avoid the possible long-term maldifferentiation of engrafted cells [11] or tumour generation [47].

(See related article by Ratajczak et al. The emerging role of microvesicles in cellular therapies for organ/tissue regeneration. *Nephrol Dial Transplant* 2011; 26: 1453–1455.)

References

1. Uccelli A, Moretta L, Pistoia V. Mesenchymal stem cells in health and disease. *Nat Rev Immunol* 2008; 8: 726–736
2. Picinich SC, Mishra PJ, Glod J *et al*. The therapeutic potential of mesenchymal stem cells. Cell-and tissue-based therapy. *Expert Opin Biol Ther* 2007; 7: 965–973
3. Morigi M, Imberti B, Zoja C *et al*. Mesenchymal stem cells are renotropic, helping to repair the kidney and improve function in acute renal failure. *J Am Soc Nephrol* 2004; 415: 1794–1804
4. Herrera MB, Bussolati B, Bruno S *et al*. Mesenchymal stem cells contribute to the renal repair of acute tubular epithelial injury. *Int J Mol Med* 2004; 14: 1035–1041
5. Tögel F, Hu Z, Weiss K *et al*. Administered mesenchymal stem cells protect against ischemic acute renal failure through differentiation-independent mechanisms. *Am J Physiol Renal Physiol* 2005; 289: F31–F42
6. Lange C, Togel F, Ittrich H *et al*. Administered mesenchymal stem cells enhance recovery from ischemia/reperfusion-induced acute renal failure in rats. *Kidney Int* 2005; 68: 1613–1617
7. Semedo P, Wang PM, Andreucci TH *et al*. Mesenchymal stem cells ameliorate tissue damages triggered by renal ischemia and reperfusion injury. *Transplant Proc* 2007; 39: 421–423
8. Morigi M, Introna M, Imberti B *et al*. Human bone marrow mesenchymal stem cells accelerate recovery of acute renal injury and prolong survival in mice. *Stem Cells* 2008; 26: 2075–2082
9. Ninichuk V, Gross O, Segerer S *et al*. Multipotent mesenchymal stem cells reduce interstitial fibrosis but do not delay progression of chronic kidney disease in collagen4A3-deficient mice. *Kidney Int* 2006; 70: 121–129
10. Prodromidi EI, Poulsom R, Jeffery R *et al*. Bone marrow-derived cells contribute to podocyte regeneration and amelioration of renal disease in a mouse model of Alport syndrome. *Stem Cells* 2006; 24: 2448–2455
11. Kunter U, Rong S, Boor P *et al*. Mesenchymal stem cells prevent progressive experimental renal failure but maldifferentiate into glomerular adipocytes. *J Am Soc Nephrol* 2007; 18: 1754–1764
12. Semedo P, Correa-Costa M, Antonio Cenedeze M *et al*. Mesenchymal stem cells attenuate renal fibrosis through immune modulation and remodelling properties in a rat remnant kidney model. *Stem Cells* 2009; 27: 3063–3073
13. Choi S, Park M, Kim J *et al*. The role of mesenchymal stem cells in the functional improvement of chronic renal failure. *Stem Cells Dev* 2009; 18: 521–529
14. Choi SJ, Kim JK, Hwang SD. Mesenchymal stem cell therapy for chronic renal failure. *Expert Opin Biol Ther* 2010; 10: 1217–1226
15. Togel F, Weiss K, Yang Y *et al*. Vasculotropic, paracrine actions of infused mesenchymal stem cells are important to the recovery from acute kidney injury. *Am J Physiol Renal Physiol* 2007; 292: F1626–F1635
16. Bi B, Schmitt R, Israilova M *et al*. Stromal cells protect against acute tubular injury via an endocrine effect. *J Am Soc Nephrol* 2007; 18: 2486–2496
17. Imberti B, Morigi M, Tomasoni S *et al*. Insulin-like growth factor-1 sustains stem cell-mediated renal repair. *J Am Soc Nephrol* 2007; 18: 2921–2928
18. Tögel F, Zhang P, Hu Z *et al*. VEGF is a mediator of the renoprotective effects of multipotent marrow stromal cells in acute kidney injury. *J Cell Mol Med* 2009; 13: 2109–2114
19. Liu KD, Brakeman PR. Renal repair and recovery. *Crit Care Med* 2008; 36: S187–S192
20. Bi B, Guo J, Marlier A *et al*. Erythropoietin expands a stromal cell population that can mediate renoprotection. *Am J Physiol Renal Physiol* 2008; 295: F1017–F1022
21. Cantaluppi V, Biancone L, Romanazzi GM *et al*. Macrophage stimulating protein may promote tubular regeneration after acute injury. *J Am Soc Nephrol* 2008; 19: 1904–1918
22. Ratajczak J, Wysoczynski M, Hayek F *et al*. Membrane-derived microvesicles: important and underappreciated mediators of cell-to-cell communication. *Leukemia* 2006; 20: 1487–1495
23. Bruno S, Grange C, Deregibus MC *et al*. Mesenchymal stem cell-derived microvesicles protect against acute tubular injury. *J Am Soc Nephrol* 2009; 20: 1053–1067
24. De Broe ME, Wieme RJ, Logghe GN *et al*. Spontaneous shedding of plasma membrane fragments by human cells in vivo and in vitro. *Clin Chim Acta* 1977; 81: 237–245
25. Heijnen HF, Schiel AE, Fijnheer R *et al*. Activated platelets release two types of membrane vesicles: microvesicles by surface shedding and exosomes derived from exocytosis of multivesicular bodies and alpha-granules. *Blood* 1999; 94: 3791–3799
26. Siekevitz P. Biological membranes: the dynamics of their organization. *Annu Rev Physiol* 1972; 34: 117–140
27. Schorey JS, Bhatnagar S. Exosome function: from tumor immunology to pathogen biology. *Traffic* 2008; 9: 871–881
28. Morel O, Toti F, Hugel B *et al*. Cellular microparticles: a disseminated storage pool of bioactive vascular effectors. *Curr Opin Hematol* 2004; 11: 156–164
29. Ratajczak J, Miekus K, Kucia M *et al*. Embryonic stem cells-derived microvesicles reprogram hematopoietic progenitors: evidence for horizontal transfer of mRNA and protein delivery. *Leukemia* 2006; 20: 847–856
30. Deregibus MC, Cantaluppi V, Calogero R *et al*. Endothelial progenitor cell-derived microvesicles activate an angiogenic program in endothelial cells by a horizontal transfer of mRNA. *Blood* 2007; 110: 2440–2448
31. Valadi H, Ekström K, Bossios A *et al*. Exosome-mediated transfer of mRNAs and microRNAs is a novel mechanism of genetic exchange between cells. *Nat Cell Biol* 2007; 9: 654–659
32. Herrera MB, Fonsato V, Gatti S *et al*. Human liver stem cell-derived microvesicles accelerate hepatic regeneration in hepatectomized rats. *J Cell Mol Med* 2009; 14: 1605–1618
33. Yuan A, Farber EL, Rapoport AL *et al*. Transfer of microRNAs by embryonic stem cell microvesicles. *PLoS One* 2009; 4: e4722
34. Quesenberry PJ, Aliotta JM. The paradoxical dynamism of marrow stem cells: considerations of stem cells, niches, and microvesicles. *Stem Cell Rev* 2008; 4: 137–147
35. Aliotta JM, Sanchez-Guijo FM, Dooner GJ *et al*. Alteration of marrow cell gene expression, protein production, and engraftment into lung by lung-derived microvesicles: a novel mechanism for phenotype modulation. *Stem Cells* 2007; 25: 2245–2256
36. Quesenberry PJ, Dooner MS, Aliotta JM. Stem cell plasticity revisited: the continuum marrow model and phenotypic changes mediated by microvesicles. *Exp Hematol* 2010; 38: 581–592
37. Aliotta JM, Pereira M, Johnson KW *et al*. Microvesicle entry into marrow cells mediates tissue-specific changes in mRNA by direct delivery of mRNA and induction of transcription. *Exp Hematol* 2010; 38: 233–245
38. Granot D, Kunz-Schughart LA, Neeman M. Labeling fibroblasts with biotin-BSA-GdDTPA-FAM for tracking of tumor-associated stroma by fluorescence and MR imaging. *Magn Reson Med* 2005; 54: 789–797
39. Collino F, Deregibus MC, Bruno S *et al*. Microvesicles derived from adult human bone marrow and tissue specific mesenchymal stem cells shuttle selected pattern of miRNAs. *PLoS One* 2010; 5: e11803

40. Gnecchi M, Zhang Z, Ni A *et al*. Paracrine mechanisms in adult stem cell signaling and therapy. *Circ Res* 2008; 103: 1204–1219

41. Caplan AI, Dennis JE. Mesenchymal stem cells as trophic mediators. *J Cell Biochem* 2006; 98: 1076–1084

42. Humphreys BD, Valerius MT, Kobayashi A *et al*. Intrinsic epithelial cells repair the kidney after injury. *Cell Stem Cell* 2008; 2: 284–291

43. Vogetseder A, Picard N, Gaspert A *et al*. The proliferation capacity of the renal proximal tubule involves the bulk of differentiated epithelial cells. *Am J Physiol Cell Physiol* 2008; 294: C22–C28

44. Mause SF, Weber C. Microparticles, protagonist of a novel communication network for inter cellular information exchange. *Circ Res* 2010; 107: 1047–1057

45. Semedo P, Donizetti-Oliveira C, Burgos-Silva M *et al*. Bone marrow mononuclear cells attenuate fibrosis development after severe acute kidney injury. *Lab Invest* 2010; 90: 685–695

46. Alexandre CS, Volpini RA, Shimizu MH *et al*. Lineage. -negative bone marrow cells protect against chronic renal failure. *Stem Cells* 2009; 27: 682–692

47. Thirabanjasak D, Tantiwongse K, Thorner PS. Angiomyeloproliferative lesions following autologous stem cell therapy. *J Am Soc Nephrol* 2010; 21: 1218–1222

Activated human renal tubular cells inhibit autologous immune responses

Ray Wilkinson[1,2,3], Xiangju Wang[1,2], Kathrein E. Roper[1,2] and Helen Healy[1,2,3]

[1]Conjoint Renal Laboratory, Pathology Queensland, [2]Department of Renal Medicine, Royal Brisbane and Women's Hospital, Brisbane, Australia and [3]Medical School, University of Queensland, Brisbane, Australia

Correspondence and offprint requests to: Ray Wilkinson; E-mail: ray.wilkinson@qimr.edu.au

Abstract

Background. Renal proximal tubule epithelial cells (PTEC) respond and contribute to the pathological process in a range of kidney diseases. Within this disease setting, PTEC up-regulate surface antigens which may enable them to act as non-professional antigen-presenting cells and become targets for infiltrating T cells in the context of disease and allograft rejection. In order to define, for the first time, whether PTEC modulate immune responses within the autologous human system, we monitored their interaction with T and B cells in the presence of stimuli which mimic immunological signalling.

Methods. The expression of PTEC surface antigen in response to inflammatory mediators was monitored by flow cytometry. Purified T and B lymphocyte subsets and peripheral blood mononuclear cells were cultured in the presence or absence of autologous activated PTEC, and their responses to specific activators were monitored by proliferation, cytokine secretion and surface antigen expression. Some experiments were performed in the presence of blocking antibodies to PD-L1.

Results. The presence of activated primary autologous PTEC resulted in significantly decreased T- and B-cell proliferative responses, which were only partly mediated by programmed death ligand 1. This modulation was not induced by a decrease in activation markers or an increase in T regulatory cells but was accompanied by strong significant skewing of cytokine profiles. Significant decreases in gamma-interferon, interleukin-2 and tumour necrosis factor and increases in interleukin-4 were detected in the presence of PTEC, indicating that these cells induce a shift away from an inflammatory Th1 effector profile to a Th2 type profile.

Conclusion. Human PTEC do modulate autologous immune responses. We hypothesize that such mechanisms may have developed to help dampen inflammatory responses and macrophage activation seen within kidney interstitium in many immune-mediated kidney diseases.

Keywords: immune modulation; proximal tubule epithelial cells

Introduction

Proximal tubule epithelial cells (PTEC) of the kidney are known to respond to and mediate the disease process in a wide range of kidney diseases [1–4]. Many of the chemokines secreted by PTEC in the perturbed disease state, including transforming growth factor beta (TGF-β), RANTES, MCP-1 and IL-8, result in a pro-inflammatory phenotype within the interstitium of the kidney. This attracts